RSC Advances

RSC Advances

www.rsc.org/advances

ROYAL SOCIETY OF CHEMISTRY

www.rsc.org/advances

Journal Name

ARTICLE

Facile and surfactant-free synthesis of supported Pd nanoparticles on hydrotalcite for oxidation of benzyl alcohol

Yufei He, Pengfei Yang, Jiaxuan Fan, Yanan Liu, Yiyun Du, Junting Feng*, Faying Fan and Dianqing Li*

We report a facial modified-deposition-precipitation method which permits reproducible preparation of supported Pd catalyst possessing small particle size and tight size distribution but without protection of surfactant and any additional treatment. The value of pH in this technique plays a key role to control the size of Pd nanoparticles as well as the electronic environment of surface Pd atoms. With the increasing pH (4. 0~12.0), the average size of Pd nanoparticles decreases gradually, meanwhile, the peak area ratio for CO adsorbed on bridge-bonded Pd to that adsorbed on threefold-coordinate Pd increases. Stronger support-metal interaction (electron transfer from Pd^0 to support) is observed at pH of 7.0 and 10.0. Both the small particle size and the electron-deficient surface metallic Pd contribute to the enhancement in the activity in the solvent-free oxidation of benzyl alcohol. Therefore, compared with supported Pd catalysts prepared by sol-immobilization, impregnation and deposition-precipitation methods, Pd/hydrotalcite synthesized by this modified-deposition-precipitation approach shows a higher TOF value (5330 h^{-1}). This preferred catalytic performance can also be maintained in five cycle runs. Under the consideration of green chemistry, a number of Pd catalysts were then prepared on alternative supports using this method without the addition of alkali in the preparation process.

1. Introduction

Supported Pd nanoparticles have been found to be effective for amount of applications, including energy processing,[1,2] aerobic oxidation reaction,[3,4] hydrogenation reaction,[5,6] carbon-carbon coupling,[7,8] oxygen reduction reaction [9,10] as well as environmental catalysis.[11-13] To achieve the highest activity and selectivity, it is desirable to have uniform dispersed nanoparticles (NPs) which have identical properties and distribution. Many methods for preparing highly active heterogeneous Pd catalysts have been reported to date such as impregnation,[14] deposition-precipitation,[15] sol-immobilization or colloidal

deposition,[16] ligand-assisted synthesis,[17] chemical vapor deposition.[18] Conventional synthesis approaches do not provide the requisite degree of control, since they start from Pd salts which are first deposited on a support by precipitation or impregnation. Reduction of these methods is achieved by high-temperature treatments involving calcination and H_2 reduction, leading to the aggregation of the resulting particles. The obtained Pd catalysts then displayed only a moderate level of activity in, for example, the direct synthesis of hydrogen peroxide or the solvent-free oxidation of alcohols.[19,20] Hence, there has been considerable interest in developing colloidal routes to

synthesize highly dispersed heterogeneous catalysts. In the process of colloidal methods, polymer protecting agents such as polyvinyl pyrrolidone (PVP) and polyvinyl alcohol (PVA) are generally employed to stabilize the size as well as the shape of metal colloids.[21-23] These polymer-capped NPs have shown preferred activity in a variety of liquid-phase reactions.[24,25] However, the capping agent must be removed to achieve high catalytic activity, and the high-temperature treatments used for removal the capping agent would lead to particle aggregation and loss of monodispersity.[26,27] Therefore, considerable effort is still being expended to discover a facile and effective method for the reproducible preparation of highly active and stable supported Pd NPs catalysts.

Recent work by Hutchings' group [28] has shown that a modification and post-reduction step to the impregnation method to prepare supported AuPd/TiO$_2$ catalyst possessing a tight Au particle size distribution of 2-5 nm but without the ligands adsorbed on the particle surface. Similarly, by the precise control of the precipitation condition, Pd nanoparticles with narrow size distribution (2-4 nm) was synthesized [29], even on low-surface-area inorganic powders [30]. Moreover, Datye et al. [31] reported a Pd/C catalyst with 1.5 nm NPs by the reduction of palladium acetate in methanol under anhydrous conditions. Additionally, Gatica and co-worker [32] prepared Au supported on ceria–zirconia mixed oxides using a speciation-controlled incipient wetness impregnation approach, and the resulting NPs featured both high gold loadings and excellent metal dispersions. Thus it can be seen that well-dispersed NPs could be synthesized by the precise tuning of preparation condition based on the existing approaches.

In previous study, hydrotalcite (HT), a type of two-dimensional (2D) layered inorganic material, has exhibited an increased catalytic performance in the oxidation reactions owing to the tunable acidity-basicity of the surface.[33,34] HT has the general formula [M$^{2+}_{1-x}$M$^{3+}_{x}$(OH)$_2$]$^{x+}$(A^{n-})$_{x/n}$·mH$_2$O, where M^{2+} and M^{3+} indicate metallic cations, x is the molar ratio of M^{3+}/(M^{2+}+M^{3+}), A^{n-} represents the interlayer anion and m indicates the amount of water.[35,36] Besides the acidity-basicity, HT also offers the cation-tunability of the brucite-like layers as well as the high adsorption capacity, which make it extensively investigated in the field of both fundamental research and practical process. [37,38] For example, a green preparation of Pt NPs has been developed using soluble starch as a reducing and stabilizing agent and the Pt NPs were then immobilized on an MgAl-LDH surface.[39] These Pt/HT catalysts were employed in the oxidation of glycerol in water and showed 41% yield and 75% selectivity for glyceric acid with a turnover number of 357. In addition, our group reported a series of LDH-supported Pd catalysts for the partial hydrogenation of acetylene, which showed an enhanced catalytic performance.[40-42] Therefore, synthesis of HT supported Pd catalysts with small particle size and narrow size distribution is of great importance to gain insight of HT supported catalysts as well as to broaden its potential industrial application.

In this work, we describe a facial route for synthesizing highly dispersed Pd/HT catalyst that involves the reduction of Pd(II) by NaBH$_4$. The value of pH is vital to obtain a well-dispersed Pd NPs on the HT support. It is worth noted that the preparation is conducted under room temperature and no capping agent as well as thermal treatment is required in this process. High-resolution transmission electron microscope and CO chemical pulse are used to determine the size and dispersion of the resulting Pd NPs. The status and electronic environment of surface Pd atoms are revealed by the CO-IR and X-ray photoelectron spectroscopy analysis. Additionally, this technique is extended to other powder supports (HT with different Mg/Al ratios, MgO and hydroxyapatite (HAP)). These catalysts are also found to be active, very selective to

RSC Advances

benzaldehyde and stable for solvent-free aerobic oxidation of benzyl alcohol (BA).

2. Experimental

2.1 Support preparation

The Mg_2Al-HT compound was prepared by co-precipitation at pH = 10.0 (± 0.1) of suitable amounts of $Mg(NO_3)_2 \cdot 6H_2O$ (7.38 g) and $Al(NO_3)_3 \cdot 6H_2O$ (5.40 g) with solutions of NaOH (1 M) and Na_2CO_3 (0.4 M). The addition of the alkaline solution and pH were controlled by pH meter (Mettler-Toledo FE20). The suspension was stirred at 353 K for 6 h, and the precipitate was then centrifuged and thoroughly washed with deionized water until the pH reached 7.0. After drying 12 h at 383 K, the Mg_2Al-HT support was obtained. Other MgAl-HT materials with different Mg/Al molar ratios (Mg_3Al-HT Mg_4Al-HT and Mg_5Al-HT) were prepared by the same method by adjusting the amounts of $Mg(NO_3)_2 \cdot 6H_2O$ and NaOH($[Mg^{2+}]+[Al^{3+}]/[OH^-]=1.6$).

2.2 Catalysts preparation

2.2.1 Supported Pd catalysts on HT by modified-deposition-precipitation (MDP) method

1.00 g Mg_2Al-HT support was first suspended in 50 ml aqueous solution. The pH value of the suspension was controlled by the addition of NaOH (0.1 M). Until the pH reached 10.0, 2 ml Na_2PdCl_4 (0.046 M) was poured into the suspension. After that, more NaOH solution was added to maintain the overall pH at 10.0. A freshly prepared solution of $NaBH_4$ (0.1M, $NaBH_4$/Pd (mol/mol)=5) was then added and the solution turned into dark-brown. After another 1 h stirring, the precipitate was centrifuged and thoroughly washed with deionized water until the pH ~ 7.0. The washed solid was dried (383 K for 12 h) and the obtained catalyst was donated as Pd/HT$_{MDP-10}$. A variation in the MDP procedure was also investigated. The preparation process kept the same except for the control of pH value. When the pH was set at 12.0, the obtained catalyst was donated as Pd/HT$_{MDP-12}$. The catalyst was also

prepared under the acid condition (donated as Pd/HT$_{MDP-4}$), in which the pH was adjusted by the addition of HCl (0.1 M) to 4.0. Moreover, the Pd/HT catalyst without the adjustment of pH was donated as Pd/HT$_{MDP-7}$.

Using the same method, Pd/Mg_3Al-HT, Pd/Mg_4Al-HT, Pd/Mg_5Al-HT, Pd/MgO and Pd/ hydroxyapatite were also prepared.

2.2.2 Supported Pd catalysts on HT by other methods

As comparison, supported Pd catalysts on HT were prepared using other three preparation methods: impregnation (donated as Im), deposition-precipitation (DP) and sol-immobilisation (SIm). The detailed procedures for the three preparation methods have been described in detail elsewhere.[14-16] Briefly, for the synthesis of Pd/HT prepared by impregnation is as follow: 1.4 ml Na_2PdCl_4 (0.046 M) was added in a stirred and heated aqueous solution (10 ml). The resultant solution was then added to the Mg_2Al-HT (1.00 g) and the resulting slurry was dried at 383 K for 12 h. The resulting powder was ground and calcined in static air (673 K, 4 h) followed by reduction in 10% H_2/Ar (473 K, 2 h). This material was designated Pd/HT$_{Im}$. In case of DP method, a stirred, slurry of Mg_2Al-HT (1.00 g) in water (50 ml) was adjusted to pH 10 by the dropwise addition of (0.1 M) NaOH. 1.4 ml Na_2PdCl_4 (0.046 M) was added in the suspension and NaOH was added dropwise to maintain the overall pH at 10 for 1 h. The slurry was then filtered, washed with deionized water. The washed solid was dried (383 K for 12 h) and calcined in air (673 K, 4 h) and reduced in H_2/Ar (473 K, 2 h). This material was designated Pd/HT$_{DP}$. As for sol-immobilization method. To an aqueous fresh Na_2PdCl_4 solution, the required amount of a PVA solution (1 wt.%) was added (PVA/Pd (wt./wt.)=1.2); a freshly prepared solution of $NaBH_4$ (0.1M, $NaBH_4$/Pd (mol./mol.)=5) was then added to form a dark-brown sol. After 1 h of sol generation, the colloid was immobilized by adding Mg_2Al-HT (1.00 g) under vigorous stirring conditions. After

another 1 h the slurry was filtered, the catalyst washed thoroughly with deionized water and dried at 383 K for 12 h. The obtained catalyst was donated as Pd/HT$_{SIm}$.

2.3 Catalyst characterization

The specific surface area was calculated according to the Brunauer-Emmett-Teller (BET) method based on the adsorption isotherm. Elemental analysis for Pd was recorded using a Shimadzu ICPS-75000 inductively coupled plasma atomic emission spectrometer (ICP-AES). The morphology and size of the samples were examined using a JEOL JEM-2100F high-resolution transmission electron microscope (HRTEM). CO pulse chemisorption was conducted at 110 °C on a Micrometric ChemiSorb 2920 equipped with 50 μl loop. XRD analysis of supported Pd catalysts performed on a Shimadzu XRD-6000 diffractometer using Cu K$_{\alpha}$ radiation (λ = 0.154 nm) in the 2θ range of 3-70° with a scan speed of 10° min^{-1}. X-ray photoelectron spectra (XPS) of the samples were collected using a Thermo VG ESCALAB 250 spectrometer equipped with a Mg K$_{\alpha}$ anode. The C 1s peak at 284.6 eV was used for calibration. In situ diffuse reflectance infrared Fourier transform spectroscopy (DRIFTS) was performed on a Bruker Tensor 27 instrument. The sample was pressed into a self-supporting pellet and pretreated in the same cell used for the measurement. After hydrogen reduction and nitrogen pretreatment at 373 K for 30 min, the DRIFTS spectrum of the catalyst was recorded at 3 mbar with a resolution of 4 cm^{-1} in order to obtain a background spectrum. Then the catalyst was exposed to a CO flow for 30 min. DRIFTS measurements of CO chemisorbed on catalysts were conducted after the pressure was reduced to 3 mbar.

2.4 Alcohol oxidation

The catalytic performance was evaluated by the solvent-free aerobic oxidation of benzyl alcohol which was carried out in a 50 ml glass reactor under the O$_2$ pressure at 1 bar. In a typical reaction, 3 ml benzyl alcohol and the requisite amount of catalyst (alcohol/active mental molar ratio was 10000) were added. The air in the reactor was exhausted by ultrahigh purity O$_2$ flow for about 1 min and the O$_2$ was continuously delivered to keep the pressure at 1 bar during the reaction. The reactor was then kept in a heating block which was preheated to 373K and the mixture was stirred at the speed of 1000 rpm. After a specific time, the samples were rapidly cooled in a cold water bath and centrifuged to remove the solid catalyst.

An aliquot of the clear supernatant reaction mixture (0.5 ml) was diluted with mesitylene (0.5 ml, external standard for GC analysis). For the analysis of the products an Agilent J&W GC-FID (DB-Wax, 30 m × 0.320 mm, df = 0.25 μm) were employed. The products were identified by comparison with known authentic standards. For the quantification of the amounts of reactants consumed and products generated, an external standard method was used. The selectivity was calculated as mol of product formed per mol of reacted benzyl alcohol and the carbon balance was within ± 2%.

3. Results and discussion

3.1 Characterization of Catalyst

Pd/HT catalysts prepared by the modified-deposition-precipitation method were successfully synthesized under the different pH values of 4.0, 10.0, 12.0 (Pd/HT$_{MDP-4}$, Pd/HT$_{MDP-10}$ and Pd/HT$_{MDP-12}$, repectively) as well as without pH adjustment (Pd/HT$_{MDP-7}$). BET specific surface areas of Pd catalysts prepared by MDP method are given in Table 1. The value of supported Pd catalysts under different pH is similar and reproducible within experimental error. Detailed HRTEM studies were carried out to compare the morphologies of 1 wt % Pd/HT$_{MDP}$ catalysts under different pH value. As shown in Fig. 1, the Pd NPs are evenly dispersed over the surface of HT and no obvious aggregation is observed for four catalysts. More than 200 particles in different regions are randomly

selected to measure the distribution and mean size of Pd   nanoparticles.

Table 1 The properties of Pd/HT catalysts prepared by modified-deposition–precipitation using different pH values

Sample	Surface area[a] (m^2/g)	Pd loading[b] (%)	Particle size (nm)	Theoretical dispersion[c] (%)	CO uptake[d] (µmol/g)	Dispersion [e](%)
Pd/HT$_{MDP-4}$	107	1.08	3.7	23.8	12.3	24.2
Pd/HT$_{MDP-7}$	110	1.02	2.5	35.2	22.9	47.8
Pd/HT$_{MDP-10}$	98	0.98	2.3	38.3	25.0	51.4
Pd/HT$_{MDP-12}$	103	1.02	2.2	40.0	12.4	26.9

[a] Determined by BET analysis [b] Determined by ICP analysis [c] Estimated by average particle size [d] Determined by CO pulse [e] Determined by CO uptake assuming a Pd/CO stoichiometry of 2:1

It can be clearly seen that the mean size of Pd NPs decreases (from 3.7 nm to 2.2 nm) with increasing pH value (from 4.0 to 12.0). Significantly, the size of Pd NPs larger than 6.0 nm disappears gradually and the size distribution becomes narrow with the addition of NaOH (0.5-9.0 nm for Pd/HT$_{MDP-4}$, 0.5-8.0 nm for Pd/HT$_{MDP-7}$, 0.5-6.0 nm for Pd/HT$_{MDP-10}$ and 0.5-6.0 nm for Pd/HT$_{MDP-12}$). Moreover, the percentage of Pd NPs between 1.0 and 3.0 nm apparently goes up with the increasing pH (33.0%, 73.2%, 82.7% and 85.4%). The narrow size distribution and large percentage of small NPs would contribute to the incease of activity. Interestingly, Pd NPs embedded in the edge of HT support are observed in Fig. 1B, D, E, which are regared to not only effectively prevent the NPs from migration and aggregation during use but also induce the strong metal support interaction.[43,44]

Based on the average NPs diameter determined from HRTEM, the theoretical dispersion is calculated by the formula described elsewhere.[45,46] As listed in Table 1, the dispersion of Pd catalysts increase with the decreasing NPs size. To acquire more precise value, the CO chemisorption pulse was also performed. Distinct from the theoretical value, "volcano" curve is present for the CO uptake of four catalysts. The dispersion was then calculated from the CO uptake assuming a Pd/CO stoichiometry of 2:1. The results show that the Pd/HT$_{MDP-10}$ has the highest dispersion (51.4%), followed by the Pd/HT$_{MDP-7}$ (47.8%), which is almost double that for two other catalysts. The superior dispersion of Pd/HT$_{MDP-7}$ and Pd/HT$_{MDP-10}$ could be ascribed to the small Pd NPs as well as the tight size distribution. As for Pd/HT$_{MDP-12}$, even though small Pd NPs are obtained, the low dispersion may be ascribed to the different status and electronic environment of surface Pd atoms.
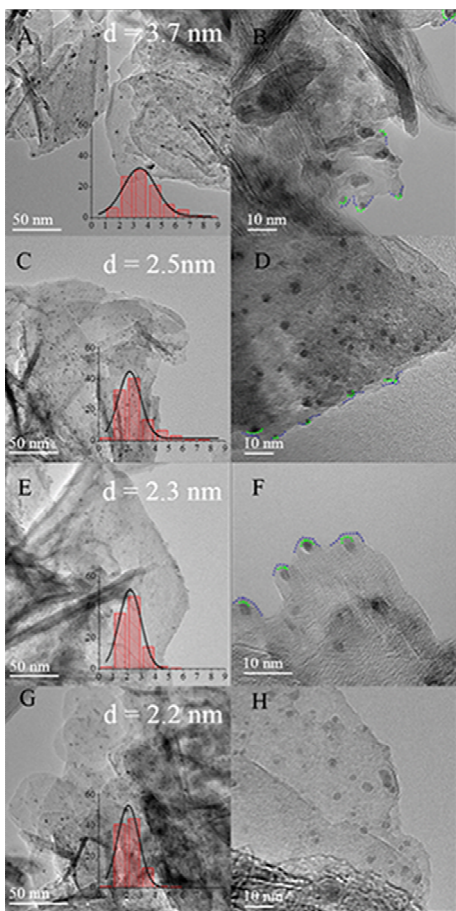
Fig. 1 HRTEM images and the size distribution of A, B) Pd/HT$_{MDP-4}$, C, D) Pd/HT$_{MDP-7}$ and E, F) Pd/HT$_{MDP-10}$ and G, H) Pd/HT$_{MDP-12}$

The extensive literatures regarding the adsorption of CO to Pd makes this molecule well suited as an infrared radiation probe of adsorption sites present on the Pd particles, therefore, in situ DRIFTS of samples exposed to CO at room temperature were performed. In Fig. 2, two main vibrational features at ca. 1910 and 1818 cm^{-1} which are reasonably ascribed to bridge-bonded CO and threefold-hollow sites CO are observed over four catalyst.[47] In addition, a weak peak at ca. 1995 cm^{-1} is seen in Pd/HT$_{MDP-4}$ and Pd/HT$_{MDP-7}$, meanwhile, a feature at ca. 2060 cm^{-1} appears in Pd/HT$_{MDP-10}$ and Pd/HT$_{MDP-12}$. The latter could be assigned to the CO linear adsorption.[48] Comparison of the peak area ratio for CO adsorbed on bridge-bonded Pd (A_b) to that adsorbed on threefold-

coordinate Pd (A_m) shows that the A_b/A_m ratio increases with rising pH value (from 0.1 to 31.9). Moreover, the shift in the CO band position is often interpreted as evidence of changes in the electronic properties of supported metals.[48,49]
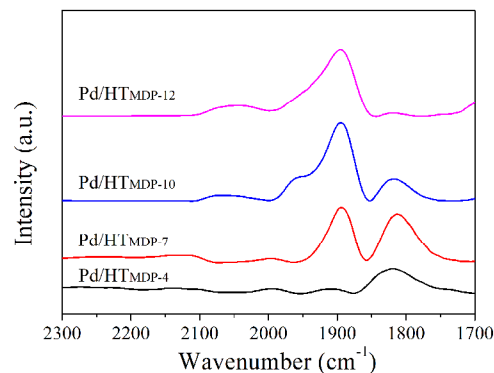

Fig. 2 In situ CO-IR spectra of A)Pd/HT$_{MDP4}$,B)Pd/HT$_{MDP-7}$, C)Pd/HT$_{MDP-10}$ and D)Pd/HT$_{MDP-12}$

In order to investigate the electronic structure of the Pd/HT catalysts under different preparation conditions, XPS analysis was carried out and the results are shown in Fig. 3. In Pd/HT$_{MDP-10}$ catalyst, the Pd 3d spectrum shows two main peaks, and the binding energy (BE) values at around 335.6 and 341.2 eV are ascribed to Pd 3d$_{5/2}$ and Pd 3d$_{3/2}$ of Pd^0.[42,49] Additionally, the peaks attributed to Pd^{2+} are also observed in the spectra. As for Pd/HT$_{MDP-7}$ catalyst, similar BE values of Pd^0 and Pd^{2+} are exhibited. Interestingly, peaks shift to lower BE by approximately 0.4 eV and 0.2 eV for Pd/HT$_{MDP-4}$ and Pd/HT$_{MDP-12}$ with respect to that of the Pd/HT$_{MDP-10}$ catalyst, suggesting distinct interaction between Pd and HT support is induced by the MDP method. As reported, the size of Pd could also affect the BE value,[50,51] however, average size of Pd NPs in Pd/HT$_{MDP-10}$ (2.3 nm) is similar with that in Pd/HT$_{MDP-12}$ (2.2 nm), this shift of Pd 3d is thus reasonably ascribed to electron transfer from Pd to the HT support, resulting in an electron-deficient surface metallic Pd, which may be favor of the enhancement in the catalytic performance.
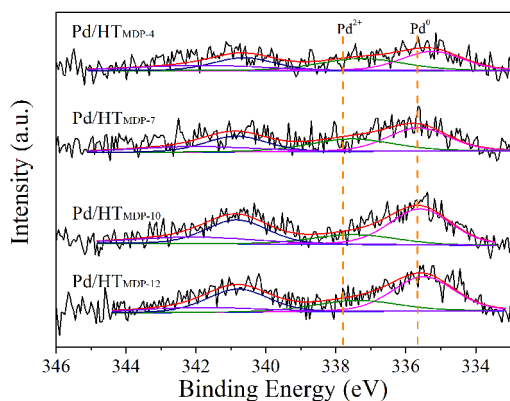
Fig. 3 XPS spectra of A)Pd/HT$_{MDP-4}$, B)Pd/HT$_{MDP-7}$, C)Pd/HT$_{MDP-10}$ and D)Pd/HT$_{MDP-12}$

3.2 Solvent-free oxidation of benzyl alcohol over Pd/HT$_{MDP}$ catalysts

The catalytic oxidation of benzyl alcohol over Pd catalysts prepared by modified-deposition-precipitation method under solvent- and base-free conditions was investigated at 373 K using a glass reactor. The results are shown in Fig. 4. The Pd/HT$_{MDP-7}$ and Pd/HT$_{MDP-10}$ catalysts exhibit a comparable conversion of BA but higher than that over Pd/HT$_{MDP-4}$ and Pd/HT$_{MDP-12}$ catalysts. Inset in Fig. 4A shows the BA conversion at 1h and 2h over four catalysts. It can be clearly seen that the BA conversion over Pd/HT$_{MDP-7}$ and Pd/HT$_{MDP-10}$ is 36.9% and 19.5% higher than that over Pd/HT$_{MDP-4}$ and Pd/HT$_{MDP-12}$, respectively, at the initial period (1 h). Similar trend is also found at the reaction time of 2 h. When the reaction extends to 6 h, the BA conversion increases to 96.8%, 94.6%, 87.3% and 83.5% for Pd/HT$_{MDP-10}$, Pd/HT$_{MDP-7}$, Pd/HT$_{MDP-12}$ and Pd/HT$_{MDP-4}$, respectively. In case of the selectivity, benzaldehyde is detected as the main product. All catalysts display high selectivity towards benzaldehyde, which is more than 94.5%. At BA conversion of 80%, a slightly higher selectivity (97.0%) is observed over Pd/HT$_{MDP-10}$ catalyst.

Based on our previous findings,[16] three-step mechanism may be involving in the oxidation of benzyl alcohol over supported metal catalysts on HT, that is, an abstraction of the proton by the hydroxyl group on the support, a β-hydride elimination on metal surface and the recovering of metallic site from metal hydride. It is speculated that the first step may determine the selectivity, meanwhile the second step is related to the activity. The elimination of β-hydride is also regarded as the rate-determining step. In our system, the employ of the same HT support with basic sites that could facilitate the abstraction of proton from benzyl alcohol leads to the high and similar selectivity towards benzaldehyde over four catalyst. As for the activity, it is generally thought that the small particles with large amount of coordinatively unsaturated metal atoms are more active for the cleavage of β-hydride, however, the highest conversion is observed over Pd/HT$_{MDP-10}$ and the conversion over Pd/HT$_{MDP-12}$ with the smallest mean size is much lower than Pd/HT$_{MDP-10}$, indicating that the activity is not only related to the particle size but also the electronic density of Pd NPs. Based on the XPS result, we speculate that an electron-deficient surface metallic Pd can contribute to cleavage β-hydride, as a result, Pd/HT$_{MDP-7}$ and Pd/HT$_{MDP-10}$ with relative small Pd NPs as well as reduced electronic density of active component exhibit the highest activity.
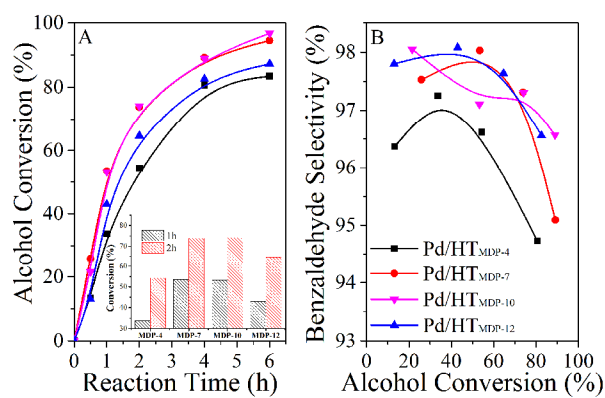

Fig. 4 Selective oxidation of benzyl alcohol over Pd/HT catalysts prepared by modified-deposition-precipitation method using different pH value: A) alcohol conversion

as a function of reaction time and B) selectivity towards benzaldehyde as a function of alcohol conversion over Pd/HT$_{MDP-4}$, Pd/HT$_{MDP-7}$, Pd/HT$_{MDP-10}$ and Pd/HT$_{MDP-12}$ catalysts. Inset in A shows the alcohol conversion at 1 h and 2 h over four catalysts. The oxidation of benzyl alcohol (3 ml) was carried out at 373 K, 1 bar pO_2, 1000 rpm stirrer speed and 10000 substrate/metal ratio.

3.3 Stability of Pd/HT$_{MDP-10}$ Catalyst

Considering both the activity and selectivity, the Pd/HT$_{MDP-10}$ catalyst possesses preferable catalytic performance in the oxidation of benzyl alcohol under our condition. To determine the efficiency of this catalyst, five consecutive reuse experiments were performed. After 4 h of reaction, the catalyst was centrifuged, washed with acetone, and dried at 383 K. Then it was employed again for another BA oxidation reaction under the same reaction conditions. As shown in figure 5, the catalyst could be reused at least five times. Only a slightly decrease in BA conversion (8.3%) is seen in the fifth run and no remarkable change in the selectivity is observed (i.e., 95.9, 96.6, 95.9, 96.2 and 96.8% for five recycling). The Pd loading of fifth used catalyst is also detected. The value is 0.98% which is the same with that of the fresh catalyst.
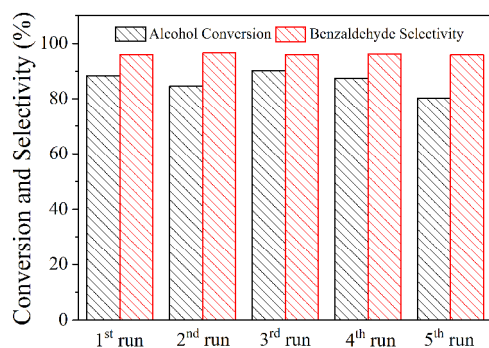
Fig. 5 Recycling of Pd/HT$_{MDP-10}$ catalyst. The oxidation of benzyl alcohol (3 ml) was carried out at 373 K, 1 bar pO_2, 4 h, 1000 rpm stirrer speed and 10000 substrate/metal ratio.

To further determine the stability of Pd/HT catalyst prepared by modified-deposition-precipitation method, the

morphology of the catalyst after five run was investigated by HRTEM. As shown in Fig. 6, Pd NPs are well dispersed on the surface of HT support and no obvious aggregation is found in the HRTEM image. The result of statistics from 200 random selected NPs shown that the average particle size is 3.0 nm. Moreover, the size distribution of used catalyst is similar with that of fresh catalyst and no larger particles (> 6.0 nm) exhibits. Therefore, we conclude that the modified-deposition-precipitation is a facile approach to synthesize the Pd/HT catalyst with small particle and tight distribution, which also shows high activity, selectivity as well as efficiency in the solvent-free oxidation of benzyl alcohol.
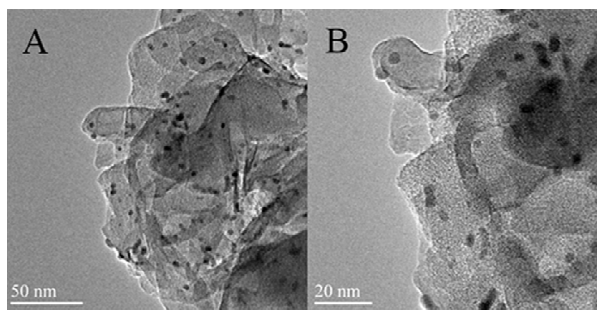
Fig. 6 HRTEM images of used Pd/HT$_{MDP-10}$ catalyst

3.4 Comparison with other preparation methods

As comparison, the supported Pd catalysts on HT are prepared by sol-immobilization, impregnation and deposition-precipitation methods. The HRTEM images of Pd/HT catalysts prepared by three approaches are shown in Fig. 7. It can be seen that the Pd NPs are well dispersed on the HT support for all the catalysts. By statistics of 200 random selected NPs, the average size and distribution are calculated. The size of Pd/HT$_{SIm}$, Pd/HT$_{Im}$ and Pd/HT$_{DP}$ is 3.6, 3.2 and 2.6 nm, respectively. Moreover, all the catalysts possess a narrow size distribution from 0.5 to 7.0 nm. However, the percentage of Pd NPs between 1.0 and 3.0 nm over these catalysts is lower than that over Pd/HT$_{MDP-10}$ catalyst. Other information about the property of Pd/HT catalysts prepared by three methods is listed in Table 2. It is highlighted that both the CO uptakes and
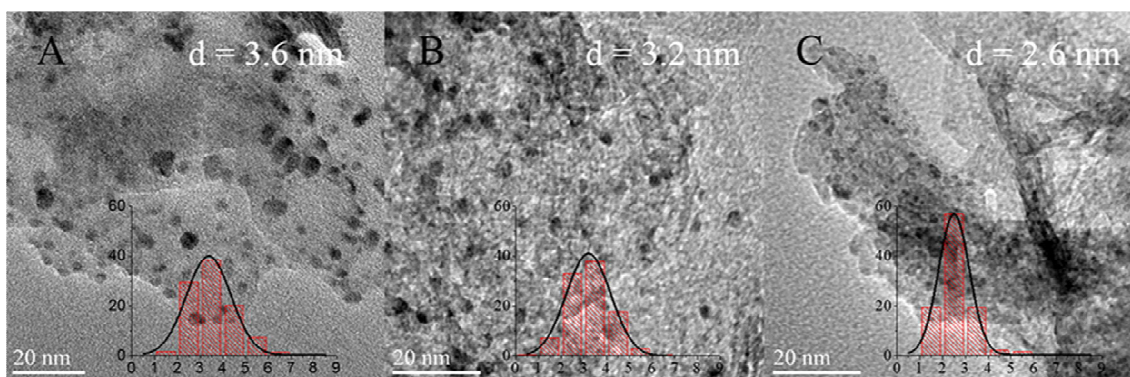
Fig. 7 HRTEM images and the size distribution of A)Pd/HT$_{SIm}$, B)Pd/HT$_{Im}$, C)Pd/HT$_{DP}$

Table 2 The properties of Pd/HT catalysts prepared by different methods

Sample	Surface area[a] (m^2/g)	Pd loading[b] (%)	Particle size (nm)	CO uptake[c] (μmol/g)	Dispersion[d] (%)	TOF[e] (h^{-1})
Pd/HT$_{Sol}$	99	1.17	3.6	10.0	21.1	4400
Pd/HT$_{Im}$	94	1.11	3.2	20.6	39.6	3000
Pd/HT$_{DP}$	104	0.95	2.6	6.8	15.8	4360
Pd/HT$_{MDP-10}$	98	0.98	2.3	25.0	51.4	5330

[a] Determined by BET analysis [b] Determined by ICP analysis [c] Determined by CO pulse [d] Determined by CO uptake assuming a Pd/CO stoichiometry of 2:1 [e] Calculated as the ratio of moles of benzyl alcohol converted per mole of total Pd per hour, measured at time-on-stream of 1 h.

corresponding dispersion of the catalysts prepared by other methods are lower than the preferable catalysts prepared by the modified-deposition-precipitation method. The increase of the particle size as well as the drop of dispersion may result in different catalytic performance.

The oxidation of benzyl alcohol was then carried out over the Pd catalysts prepared by different methods for 1 h. The results are shown in the Fig. 8. The Pd/HT$_{SIm}$ and Pd/HT$_{DP}$ possess similar BA conversion at 1 h of reaction, which is higher than that over Pd/HT$_{Im}$ catalyst. It is also seen that the Pd/HT$_{MDP-10}$ is slightly more active than the catalysts prepared by SIm and DP methods, meanwhile, it is significantly more active than that prepared by Im method. This enhanced activity can be ascribed to the small particle size and high dispersion. The selectivity to benzaldehyde is compared at the iso-conversion of BA (80%). All the Pd catalysts show a superior selectivity (more than 95%) owing to the nature of HT support. Moreover, the Pd/HT$_{DP}$ exhibits a slightly higher selectivity.
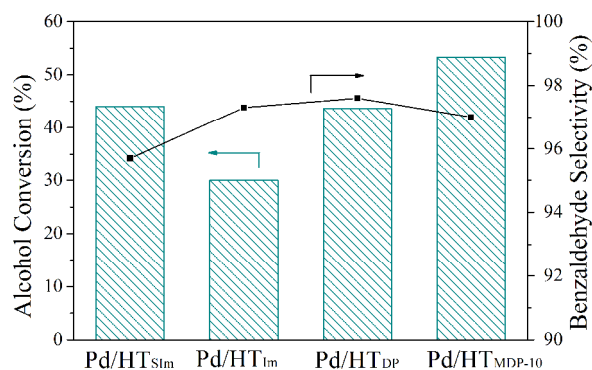
Fig. 8 Selective oxidation of benzyl alcohol over supported Pd catalysts prepared by different methods. The oxidation of benzyl alcohol (3 ml) was carried out at 373 K, 1 bar pO_2, 1000 rpm stirrer speed and 10000 substrate/metal ratio.

3.5 Pd NPs on different supports

Pd catalysts were prepared on alternative supports (e.g., HT with different Mg/Al ratios, MgO and hydroxyapatite) by this modified-deposition-precipitation method. As shown in Fig. 4, Pd/HT$_{MDP-7}$ catalyst exhibits comparable activity and a slightly lower selectivity than the best performed Pd/HT$_{MDP-10}$ catalyst. Taking into the consideration of green chemistry, these Pd catalysts on different supports were prepared without the adjustment of pH value, which avoids the addition of alkali in the preparation process. The powder XRD analysis of the obtained Pd catalysts were carried out (Fig. 9). The patterns of samples are similar to that previously reported,[16,52] suggesting the structure of the pristine support maintains under our condition. The diffraction peaks of Pd are not seen for all the catalysts due to the relatively low Pd loading and small particle size. The basicity determined by suspension of catalyst (1 g) in distilled water (50 ml) and Pd loading are listed in Table 3. Evidently, an increase in the Mg/Al atomic ratio of the HT

from 2 to 5 led to an increase of the support basicity (pH from 8.4 to 9.4), and to a decrease of Pd loading (from 1.02% to 0.96%). Moreover, Pd NPs are also successfully loaded on the surface of MgO and hydroxyapatite. The low Pd loading (0.70%) in MgO can be attributed to the formation of $Mg(OH)_2$ (seen in Fig. 9), which increase the weight of support by interaction with water in the preparation process. These data show that Pd NPs can be immobilized on the support with a pH value between 6.9 and 10.6 by this facile approach, meanwhile, the texture and nature of the support also influence preparation process.
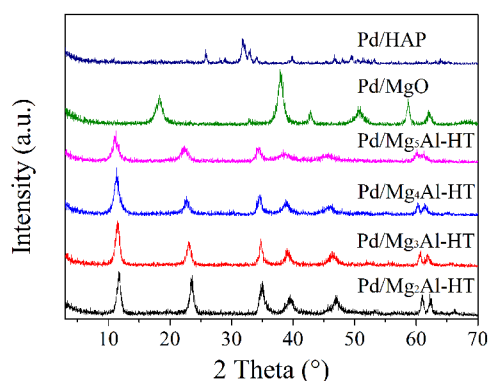

Fig. 9 XRD patterns of supported Pd catalysts prepared by modified-DP method.

The obtained catalysts were tested for the oxidation of benzyl alcohol for 1 h. The highest activity is observed over Pd/HAP catalyst, however, an obvious decrease in selectivity over this catalyst is also seen (from 98.0% to 91.4%). It is highlighted that the selectivity is calculated at the BA conversion of 57.6%, which is even lower than that obtained at conversion of 80% over Pd/HT$_{MDP-7}$ (96.4%). Moreover, the activity of catalysts drops with the increasing support basicity, indicating the catalytic performance of catalysts is truly affected by the nature of support.

Table 3 properties of Pd/HT catalysts prepared by modified-DP methods

Support	Loading[a](%)	Basicity[b] (pH)
Mg_2Al_1-LDHs	1.02	8.4
Mg_3Al_1-LDHs	1.01	8.6
Mg_4Al_1-LDHs	0.97	9.0
Mg_5Al_1-LDHs	0.96	9.4
MgO	0.70	10.6
HAP	1.04	6.9

[a] Determined by ICP analysis [b] By suspension of catalyst (1 g) in distilled water (50 ml).
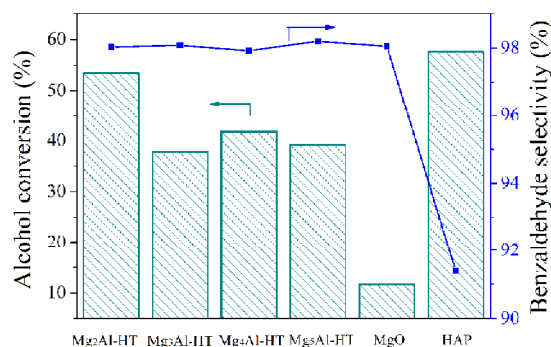

Fig. 10 The benzyl alcohol conversion and selectivity towards benzaldehyde over Pd catalysts supported on different supports prepared by MDP method at reaction time of 1 h. The oxidation of benzyl alcohol (3 ml) was carried out at 373 K, 1 bar pO_2, 1000 rpm stirrer speed and 10000 substrate/metal ratio.

4. Conclusions

A "surfactant-free", modified-deposition-precipitation methodology has been developed for preparing supported Pd/HT catalysts. Support is first suspended in the aqueous solution followed by the adjustment of pH. After the addition of active precursor in the suspension, extra NaOH or HCl is dropped to maintain the overall pH value. A freshly prepared $NaBH_4$ solution is then added quickly. The supported Pd catalysts is obtained by centrifugation and thoroughly wash. The synthesis method results in the reproducible variation of particle size and control of particle size distribution. At pH of 10, the resulting Pd NPs have an average size of 2.3 nm and 82.7% NPs are in the range of 1.0-3.0 nm. The results of CO chemisorption pulse show that this catalyst has a dispersion as high as 51.4%. Distinct status and electronic environment of surface Pd atoms under controllable pH are also revealed by the CO-IR and XPS analysis. CO-IR results show that the A_b/A_m ratio increases from 0.1 to 31.9 with rising pH value (from 4.0 to 12.0), meanwhile, XPS results indicate the stronger support-metal interaction at pH of 7.0 and 10.0 and thus an electron-deficient surface metallic Pd is obtained in Pd/HT_{MDP-10} and Pd/HT_{MDP-7}. In the solvent-free oxidation of benzyl alcohol, catalysts prepared by the MDP method are found to be 17%, 18% and 44% more active than those made by SIm, DP and Im methods. In recycling experiments, the Pd/HT_{MDP-10} catalyst retains high activity and no Pd loss or obvious aggregation is detected in the used catalyst. Under the consideration of green chemistry, a number of different Pd catalysts were also prepared on alternative supports without the addition of alkali in the preparation process. It is highlighted that this technique alleviates the need to pre-treat the catalyst and provides a new approach to synthesize well-dispersed

supported Pd catalysts.

References

1 B. Adams and A. Chen, *Mater. Today*, 2011, **14**, 282.

2 D. M. Alonso, S. G. Wettstein and J. A. Dumesic, *Chem. Soc. Rev.*, 2012, **41**, 8075.

3 D. I. Enache, J. K. Edwards, P. Landon, B. Solsona-Espriu, A. F. Carley, A. A. Herzing, M. Watanabe, C. J. Kiely, D. W. Knight and G. J. Hutchings, *Science*, 2006, **311**, 362.

4 P. F. Zhang, Y. T. Gong, H. R. Li, Z. R. Chen and Y. Wang, *Nat. Commun.*, 2013, **4**, 1593.

5 C. Q. Hu, D. Creaser, S. Siahrostami, H. Grönbeck, H. Ojagh and M. Skoglundh, *Catal. Sci. Technol.*, 2014, **4**, 2427.

6 Y. N. Liu, J. T. Feng, Y. F. He, J. H. Sun and D. Q. Li, *Catal. Sci. Technol.*, 2015, **5**, 1231.

7 L. X. Yin and J. Liebscher, *Chem. Rev.*, 2007, **107**, 133.

8 P. Sharma and A. P. Singh, *Catal. Sci. Technol.*, 2014, **4**, 2978.

9 G. F. Alvarez, M. Mamlouk, S. M. S. Kumar and K. Scott, *J. Appl. Electrochem.*, 2011, **41**, 925.

10 E. Antolini, S. C. Zignani, S. F. Santos and E. R. Gonzalez, *Electrochimica. Acta.*, 2011, **56**, 2299.

11 Y. Z. Li, Y. Yu, J. G. Wang, J. Song, Q. Li, M. D. Dong and C. J. Liu, *Appl. Catal. B: Environ.*, 2012, **125**, 189.

12 R. Wang, H. He, L. C. Liu, H. X. Dai and Z. Zhao, *Catal. Sci. Technol.*, 2012, **2**, 575.

13 S. Iqbal, X. Liu, O. F. Aldosari, P. J. Miedziak, J. K. Edwards, G. L. Brett, A. Akram, G. M. King, T. E. Davies, D. J. Morgan, D. K. Knight and G. J. Hutchings, *Catal. Sci. Technol.*, 2014, **4**, 2280.

14 L. H. Xiao, K. P. Sun, X. L. Xu and X. N. Li, *Catal. Commun.*, 2005, **6**, 796.

15 P. J. Miedziak, Q. He, J. K. Edwards, S. H. Taylor, D. W. Knight, B. Tarbit, C. J. Kiely and G. J. Hutchings, *Catal. Today*, 2011, **163**, 47.

16 J. T. Feng, C. Ma, P. J. Miedziak, J. K. Edwards, G. L. Brett, D. Q. Li, Y. Y. Du, D. J. Morgan and G. J. Hutchings, *Dalton Trans.*, 2013, **42**, 14498.

17 F. -M. McKenna, L. Mantarosie, R. P. K. Wells, C. Hardacreb and J. A. Anderson. *Catal. Sci. Technol.*, 2012, **2**, 632.

18 M. Okumura, S. Nakamura, S. Tsubota, T. Nakamura, M. Azum and M. Haruta, *Catal. Lett.*, 1998, **51**, 53.

19 J. K. Edwards, B. Solsona, A. F. Carley, A. A. Herzing, C. J. Kiely and G. J. Hutchings, *Science*, 2009, **323**, 1037.

20 P. Miedziak, M. Sankar, N. Dimitratos, J. A. Lopez-Sanchez, A. F. Carley, D. W. Knight, S. H. Taylor, C. J. Kiely and G. J. Hutchings, *Catal. Today,* 2011, **164**, 315.

21 T. Teranishi and M. Miyake, *Chem. Mater.* 1998, **10**, 594.

22 J. S. Bradley, E.W. Hill, B. Chaudret and A. Duteil, *Langmuir,* 1995, **11**, 693.

23 L. Kesavan, R. Tiruvalam, M. H. A. Rahim, M. I. bin Saiman, D. I. Enache, R. L. Jenkins, N. Dimitratos, J. A. Lopez-Sanchez, S. H. Taylor, D. W. Knight, C. J. Kiely and G. J. Hutchings, *Science*, 2011, **331**, 195.

24 H. Hirai and J. Macromol. *Sci. Part A: Pure Appl. Chem.*, 1979, **13**, 633.

25 M. Mifsud, K. V. Parkhomenko, I. W. Arends and R. A. Sheldon, *Tetrahedron*, 2010, **66**, 1040.

RSC Advances Accepted Manuscript

26 J. Park, C. Aliaga, J. Renzas, H. Lee and G. Somorjai, *Catal. Lett.*, 2009, **129**, 1.

27 A. Gniewek, J. J. ZiÓlkowski, A. M. Trzeciak, M. Zawadzki, H. Grabowska and J. Wrzyszcz, *J. Catal.*, 2008, **254**, 121.

28 M. Sankar, Q. He, M. Morad, J. Pritchard, S. J. Freakley, J. K. Edwards, S. H. Taylor, D. J. Morgan, A. F. Carley, D. W. Knight, C. J. Kiely and G. J. Hutchings, *ACS Nano*, 2012, **6**, 6600.

29 G. Agostini, R. Pellegrini, G. Leofanti, L. Bertinetti, S. Bertarione, E. Groppo, A Zecchina, and C. Lamberti *J. Phys. Chem. C*, 2009, **113**, 10485.

30 M. A. Kulagina, E.Yu. Gerasimov, T.Yu. Kardash, P.A. Simonov, A.V. Romanenko, *Catalysis Today*, 2015, **246**, 72.

31 P. D. Burton, T. J. Boyle b, A. K. Datye, *J. Catal.*, 2011, **280,** 145.

32 E. Río, D. Gaona, J. C. Hernández-Garrido, J. J. Calvino, M. G. Basallote, M. J. Fernández-Trujillo, J. A. Pérez-Omil and J. M. Gatica. *J. Catal.*, 2014, **318**, 119.

33 K. Nagashima, T. Mitsudome, T. Mizugaki, K. Jitsukawa and K. Kaneda. *Green Chem.*, 2010, **12**, 2142.

34 S. Nishimura, A. Takagaki and K. Ebitani, *Green Chem.*, 2013, **15**, 2026.

35 Y. Kuroda, Y. Miyamoto, M. Hibino, K. Yamaguchi, and N. Mizuno, *Chem. Mater.,* 2013, **25**, 2291.

36 P. J. Sideris, U. G. Nielsen, Z. Gan and C. P. Grey, *Science*, 2008, **321**, 113.

37 J. T. Feng, Y. F. He, Y. N. Liu, Y. Y. Du and D. Q. Li, *Chem. Soc. Rev.*, 2015, DOI: 10.1039/C5CS00268K.

38 G. L. Fan, F. Li, D. G. Evans and X. Duan, *Chem. Soc. Rev.*, 2014, **43**, 7040.

39 D. Tongsakul, S. Nishimura, C. Thammacharoen, S. Ekgasit and K. Ebitani, *Ind. Eng. Chem. Res.*, 2012, **51**, 16182.

40 X. Y. Ma, Y. Y. Chai, D. G. Evans, D. Q. Li and J. T. Feng, *J. Phys. Chem. C*, 2011, **115,** 8693.

41 J. T. Feng, X. Y. Ma, D. G. Evans and D. Q. Li, *Ind. Eng. Chem. Res.*, 2011, **50**, 1947.

42 Y. F. He, L. L. Liang, Y. N. Liu, J. T. Feng, C. Ma and D. Q. Li, *J. Catal.*, 2014, **309**, 166.

43 L. Guo, W. J. Jiang, Y. Zhang, J. S. Hu, Z. D. Wei and L. J. Wan, *ACS Catal.*, 2015, **5**, 2903.

44 A. H. Lu, W. C. Li, Z. S. Hou and F. Schuth, Chem. *Commun.*, 2007, 1038–1040.

45 J. R. Anderson, Structure of Metallic Catalysts, Academic Press, London, 1975.

46 Z. M. Ren, F. Zhang, L. W. Yue, X. Li, Y. Tao, G. Zhang, K. Wu, C. Wang and B. S. Li, *RSC Adv.*, 2015, **5**, 52658.

47 J. B. Giorgi, T. Schroeder, M. Bäumer and H. -J. Freund, *Surf. Sci.*, 2002, **498**, L71.

48 F. -M. McKenna and J. A. Anderson, *J. Catal.*, 2011, **281**, 231.

49 F. Cárdenas-Lizana, Y. Hao, M. Crespo-Quesada, I. Yuranov, X. Wang, M. A. Keane, and Lioubov Kiwi-Minsker, *ACS Catal.,* 2013, **3**, 1386.

50 Z. J. Zhao, F. Liu, L. M. Qiu, L. Z. Zhao and S. K. Yan, *Acta Phys. Chim. Sin.*, 2008, **24**, 1685.

51 W. P. Zhou, A. Lewera, R. Larsen, R. I. Masel, P. S. Bagus and A. Wieckowski, *J. Phys. Chem. B.*, 2006, **110**, 13393.

52 A. Ślósarczyk, Z. Paszkiewicz and C. Paluszkiewicz, *J. Mol. Struct.*, 2005, **744-747**, 657.
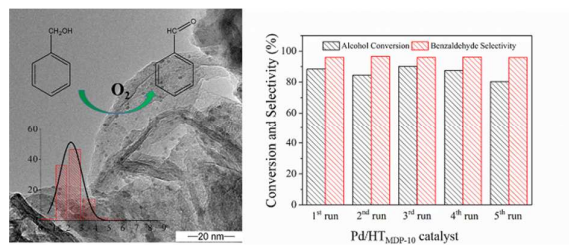
Pd/HT catalyst with an average size of 2.3 nm and an electron-deficient surface Pd is synthesized by modified-deposition-precipitation, which exhibits preferable catalytic performance in the solvent-free oxidation of benzyl alcohol.